Comparison of Higher Order FEM and MoM/SIE Approaches in Analyses of Closed- and Open-Region Electromagnetic Problems

Milan M. Ilić, Andjelija Ž. Ilić, and Branislav M. Notaroš

Abstract: We investigate the efficiency of the two most popular frequency-domain approaches in computational electromagnetics (CEM); the finite element method (FEM) and the method of moments based on the surface integral equation (MoM/SIE), both in the context of the higher order modeling. We compare the performances of the two approaches in two simple three-dimensional (3-D) problems with similar meshes, chosen as benchmark examples. The chosen examples demonstrate full-wave analysis of a wave-guiding structure (a closed-region problem) and a scatterer in free space (an open-region problem).

Keywords: Computer-aided analysis, electromagnetic analysis, finite element method, higher order elements, inhomogeneous media, method of moments.

1 Introduction

HIGHER ORDER full-wave three-dimensional (3-D) large-domain techniques in computational electromagnetics (CEM) have proven themselves to be flexible and efficient in modeling of complex structures [1–6]. The reduction in computation costs is by up to one to two orders of magnitude when compared to low order (small-domain) techniques, for the same or better accuracy. Choice of a particular numerical method such as the finite element method (FEM) or the method of moments based on the surface integral equation (MoM/SIE) is guided by the

nature of the problem at hand. FEM, where system matrices are banded and highly sparse, is often computationally more efficient. Additionally, it is considered to be the method of choice for modeling inhomogeneous media (possibly nonlinear and/or anisotropic) and geometrically versatile structures. MoM/SIE, on the other hand, is considered to be superior in dealing with open-region problems. As an answer to dealing with the complexities in modeling real world structures, where various aspects mentioned above appear all at once, hybrid FEM-MoM approaches emerge; the fields within the chosen inhomogeneous or otherwise complex domain are modeled by FEM and the domain itself is truncated by means of unknown surface currents (electric and magnetic) which are evaluated by MoM [7, 8].

Our goal in this paper is to compare the efficiency of higher order FEM and MoM/SIE techniques in the analyses of structures with inhomogeneous domains. Some practical applications where such domains are involved include electromagnetic (EM) scattering from human tissues or radar absorbing coatings, as well as scattering and diffraction from inhomogeneous dielectric lenses used in lens antennas. To the best of our knowledge, this kind of comparison has not been done before, probably because practically all of the commercially available professional software packages are based on the low order, small-domain approaches. A notable exception is WIPL-D [9].

In section 2 we briefly describe the theoretical background of the higher order FEM and MoM software implementations. In section 3 we analyze two simple problems involving inhomogeneous dielectric domains, as benchmark examples. For the comparison of approaches to be fair, we choose the examples that have the same or similar meshes in both approaches. Additionally, our choice of the two examples is such that the first example is a closed-region problem, generally more conveniently analyzed by FEM, and the second is an open-region problem, generally more conveniently analyzed by MoM. Hence, we choose the first example to feature a discontinuity in rectangular waveguide, whereas the second example analyzes a scatterer in free space.

2   Theory and Implementation

Our higher order FEM approach is based on the discretization of the curl-curl vector wave equation

$$\nabla \times \mu_{\mathrm{r}}^{-1} \nabla \times \boldsymbol{E} - k_0^2 \varepsilon_{\mathrm{r}} \boldsymbol{E} = 0, \tag{1}$$

where ε_{r} and μ_{r} are complex relative permittivity and permeability of the inhomogeneous (possibly lossy) medium, respectively, and $k_0 = \omega \sqrt{\varepsilon_0 \mu_0}$ is the free-space

wave number. Galerkin-type weak form discretization of (1) yields

$$\int_V \mu_{\mathrm{r}}^{-1} (\nabla \times \boldsymbol{e}_k) \cdot (\nabla \times \boldsymbol{E}) \, \mathrm{d}V - k_0^2 \int_V \varepsilon_{\mathrm{r}} \boldsymbol{e}_k \cdot \boldsymbol{E} \, \mathrm{d}V =$$
$$\mathrm{j} k_0 Z_0 \oint_S \boldsymbol{e}_k \cdot \boldsymbol{n} \times \boldsymbol{H} \, \mathrm{d}S, \ k = 1, ..., N_{\mathrm{FEM}}, \tag{2}$$

where V is the volume of the FEM region, S is the boundary surface of the region, $\boldsymbol{n}$ is the outward unit normal ($\mathrm{d}\boldsymbol{S} = \boldsymbol{n}\mathrm{d}S$), Z_0 is the free space impedance, and N_{FEM} is the total number of the expansion functions. Formal field-expansion used for the approximation of electric-field in (2) is

$$\boldsymbol{E} = \sum_{l=1}^{N_{\mathrm{FEM}}} \gamma_l \boldsymbol{e}_l \tag{3}$$

where $\boldsymbol{e}_l$ are the curl-conforming hierarchical polynomial basis functions [3,4], and γ_l are unknown field-distribution coefficients. The matrix form of (2) is

$$[FEM] \{\gamma\} = \mathrm{j} k_0 Z_0 \oint_S \boldsymbol{e}_k \cdot (\boldsymbol{n} \times \boldsymbol{H}) \, \mathrm{d}S. \tag{4}$$

Elements of the FEM matrix are the inner products of the employed field-expansion basis functions explicitly derived in [3] and [4]. The element type used for volume geometrical modeling in the FEM approach is the generalized curvilinear hexahedron, shown in Fig. 1. Lagrange interpolating polynomials [3] are used to define
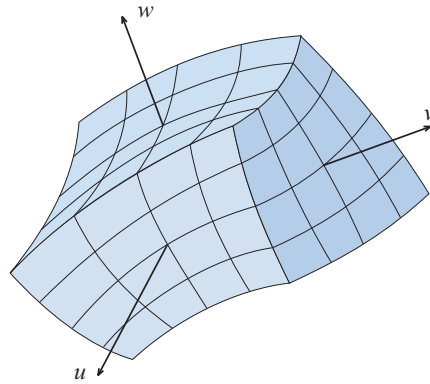

Fig. 1. Generalized curvilinear hexahedron, with local $u - v - w$ coordinates, used for volume geometric discretization in the FEM approach.

the mapping from the cubical parent domain to the Lagrange-type curved parametric hexahedron. In our examples given in Section 3, generalized hexahedral elements in FEM meshes reduce to simple bricks. The coupled electric-field integral equation/magnetic-field integral equation (EFIE/MFIE) system of equations to

be solved for electric $\boldsymbol{J}_S$ and magnetic $\boldsymbol{M}_S$ surface currents on each of the MoM surfaces, generally residing in between the two homogeneous regions with parameters ε_1, μ_1 and ε_2, μ_2, in the higher order large-domain MoM/SIE approach is

$$\left[\boldsymbol{E}(\boldsymbol{J}_S,\boldsymbol{M}_S,\varepsilon_1,\mu_1)\right]_{\mathrm{tang}} + (\boldsymbol{E}_{\mathrm{i}})_{\mathrm{tang}} = \left[\boldsymbol{E}(-\boldsymbol{J}_S,-\boldsymbol{M}_S,\varepsilon_2,\mu_2)\right]_{\mathrm{tang}}, \tag{5}$$

$$\left[\boldsymbol{H}(\boldsymbol{J}_S,\boldsymbol{M}_S,\varepsilon_1,\mu_1)\right]_{\mathrm{tang}} + (\boldsymbol{H}_{\mathrm{i}})_{\mathrm{tang}} = \left[\boldsymbol{H}(-\boldsymbol{J}_S,-\boldsymbol{M}_S,\varepsilon_2,\mu_2)\right]_{\mathrm{tang}}, \tag{6}$$

where scattered electric field $\boldsymbol{E}$ is represented by

$$\boldsymbol{E} = \boldsymbol{E}_{\mathrm{J}}(\boldsymbol{J}_S) + \boldsymbol{E}_{\mathrm{M}}(\boldsymbol{M}_S),$$
$$\boldsymbol{E}_{\mathrm{J}}(\boldsymbol{J}_S) = -\mathrm{j}\omega\boldsymbol{A} - \nabla\Phi, \quad \boldsymbol{E}_{\mathrm{M}}(\boldsymbol{M}_S) = -\frac{1}{\varepsilon}\nabla \times \boldsymbol{F}, \tag{7}$$

and scattered magnetic field $\boldsymbol{H}$ is represented by

$$\boldsymbol{H} = \boldsymbol{H}_{\mathrm{M}}(\boldsymbol{M}_S) + \boldsymbol{H}_{\mathrm{J}}(\boldsymbol{J}_S),$$
$$\boldsymbol{H}_{\mathrm{M}}(\boldsymbol{M}_S) = -\mathrm{j}\omega\boldsymbol{F} - \nabla U, \quad \boldsymbol{H}_{\mathrm{J}}(\boldsymbol{J}_S) = \frac{1}{\mu}\nabla \times \boldsymbol{A}. \tag{8}$$

The system (5)-(6) is discretized by the substitution of the formal electric and magnetic current expansions

$$\boldsymbol{J}_S = \sum_{j=1}^{N_{\mathrm{MoM}}} \alpha_j \boldsymbol{j}_{s_j}, \quad \boldsymbol{M}_S = \sum_{j=1}^{N_{\mathrm{MoM}}} \beta_j \boldsymbol{j}_{s_j}, \tag{9}$$

where $\boldsymbol{j}_{s_j}$ are the divergence-conforming hierarchical polynomial basis functions [6], into the potential equations

$$\boldsymbol{A} = \mu \int_S \boldsymbol{J}_S\, g\, \mathrm{d}S, \qquad\qquad \Phi = \frac{\mathrm{j}}{\omega\varepsilon} \int_S \nabla_S \cdot \boldsymbol{J}_S\, g\, \mathrm{d}S,$$
$$\boldsymbol{F} = \varepsilon \int_S \boldsymbol{M}_S\, g\, \mathrm{d}S, \nabla_S \cdot \boldsymbol{M}_S\, g\, \mathrm{d}S, \qquad U = \frac{\mathrm{j}}{\omega\mu} \int_S \nabla_S \cdot \boldsymbol{M}_S\, g\, \mathrm{d}S, \tag{10}$$

and solved for the values of unknown current distribution coefficients α_j and β_j, $j = 1,...,N_{\mathrm{MoM}}$, where N_{MoM} is the total number of expansion functions. In the above potential equations, g is the Green's function to be evaluated separately for each of the homogeneous regions. It is defined by

$$g = \frac{\mathrm{e}^{-\gamma R}}{4\pi R}, \quad \gamma = \mathrm{j}\omega\sqrt{\varepsilon\mu}, \tag{11}$$

where ε and μ are permittivity and permeability of the medium, respectively, and ω is the angular frequency of the implied time-harmonic variation.

The element type used for surface geometrical modeling in the MoM/SIE approach is the generalized curvilinear quadrilateral, shown in Fig. 2. Lagrange interpolating polynomials [6] are used to define mapping from the square parent domain to the Lagrange-type curved parametric quadrilateral. In our examples given in Section 3, generalized quadrilateral elements in MoM meshes reduce to simple rectangles, which also belong to the subset of bilinear quadrilaterals used for the higher order MoM/SIE modeling in WIPL-D [9].
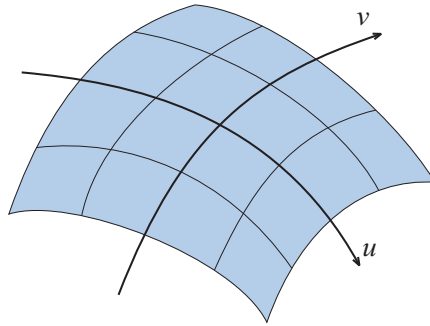

Fig. 2. Generalized curvilinear quadrilateral, with local $u-v$ coordinates, used for surface geometric discretization in the MoM/SIE approach.

3 Results and Discussion

Our extensive previous work [3,4,6], and [8], demonstrates excellent agreement of the simulation results with analytical results and/or measurements. This fact gave us confidence to base the analysis in this paper only on numerical models. All numerical results reported here are obtained using an IBM Thinkpad T60p notebook computer with Intel T7200 Core2 CPU running at 2.0 GHz under Microsoft Windows XP operating system.

As the first example, consider a dielectrically loaded WR-15 rectangular waveguide, shown in Fig. 3. The load is tightly fit inhomogeneous dielectric slab. The length of the slab and the lengths of the empty waveguide portions on both sides of the slab are the same. The slab is inhomogeneous and lossy. It consists of three equally thick layers whose real and imaginary parts of the relative permittivity ($\varepsilon_r = \varepsilon_r' - j\varepsilon_r''$) approximate a linear change from $\varepsilon_r' = 2$ to $\varepsilon_r' = 4$ and from $\varepsilon_r'' = 0.2$ to $\varepsilon_r'' = 2$, respectively, along the slab. The corresponding relative permittivities are depicted in the inset of Fig. 3. The loss-tangent in this example is rather large and ranges from $\tan\delta = 0.1$ to $\tan\delta = 0.5$ along the slab. The slab is non-magnetic. This example demonstrates analysis of a closed-region problem. For the higher order FEM approach [4], the complete loaded waveguide structure

is modeled by 5 trilinear hexahedra (bricks) which coincide with 5 waveguide sections shown in Fig. 3. Waveguide walls are considered to be lossless. The optimal polynomial orders of the field approximations, for which the solution for the modal *S*-parameters across the ports has converged, in the hexahedral elements range from 2 to 4 in different elements in different directions. This arrangement results in 231 FEM unknowns. The higher order FEM result will be compared with the solution obtained by the higher order MoM/SIE approach. MoM/SIE model is not excited by single propagating modes, but by using 2-port feeding networks. Hence, the model requires appropriate feeds as the extensions on both waveguide ports. The analyzed waveguide structure with feeds is shown in Fig. 4. The feeds consist of short-circuited waveguide sections with wire probes mounted some distance away from the short-circuited end in the middle of the waveguide. The wires have delta-function generators at the bottom ends connected to the waveguide. These generators represent structure ports 1' and 2' for which the *S*-parameters are firstly calculated and later de-embedded [9,10] to the planes of ports 1 and 2, respectively, for comparison with FEM results. Polynomial expansions for the surface currents in the MoM/SIE model are optimally chosen and they range from 1 to 6 on different surfaces in different directions. The MoM/SIE analysis of the given example is carried out using WIPL D [9].
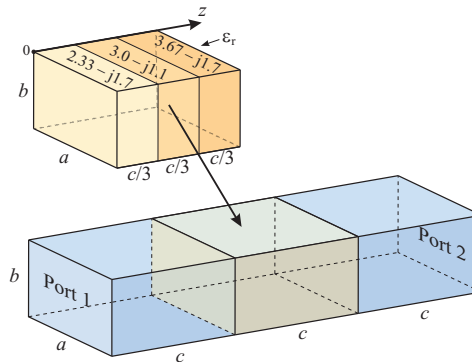

Fig. 3. Loaded WR-15 waveguide ($a = 3.76$ mm, $b = 1.88$ mm, and $c = 2.5$ mm). The load is an inhomogeneous lossy dielectric slab modeled by three equally thick homogeneous layers optimally approximating linear change of real and imaginary parts of ε_r. This is also a complete waveguide model for the FEM analysis.

In Figs. 5(a) and 5(b), the results for modal *S*-parameters of the loaded waveguide obtained by the higher order FEM are compared with those obtained by the higher order MoM/SIE approach. The results are calculated in 36 frequency points in the band of interest. Only magnitudes of S_{11} and S_{21} parameters are shown, in Figs. 5(a) and 5(b), respectively, as it was concluded that the phase characteristics do not show significant differences and thus do not carry relevant information
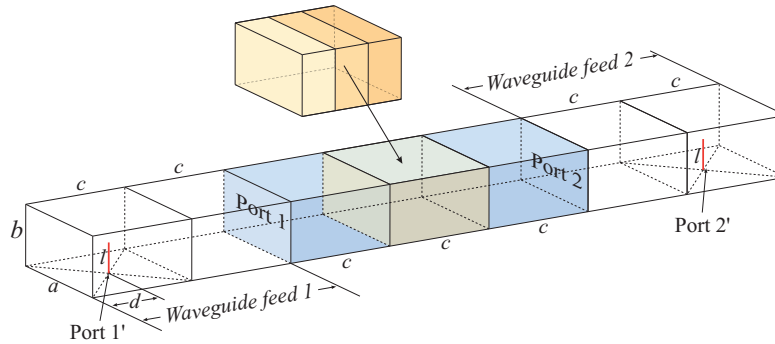
Fig. 4. Model of the loaded waveguide including short-circuited feeds with wire probes. This model is used in the MoM/SIE analysis ($d = c/2 = 1.25$ mm and $l = 1$ mm).

for comparison. Corresponding number of unknowns and simulation times for the solutions are given in the legends. We observe an excellent agreement between the FEM solution and the MoM/SIE solution. However, a significantly large number of unknowns is employed in the MoM/SIE solution, 1088, compared to only 231 unknowns in the FEM solution. This results in significantly longer simulation time required for the MoM/SIE smulation; 67 seconds compared to only 1 second required for the FEM simulation. Note that the presented MoM/SIE solution is optimal in terms of the polynomial expansion orders for currents, it has converged to the best possible solution for the given model, and it has proven to be invariant to changes of the de-embedding parameters. Additionally, the presented number of unknowns and simulation time do not include the pre-simulations of the waveguide feeds, necessary for the de-embedding process [10]. We recognize here that FEM inherently requires less computational resources than MoM/SIE for analysis of this kind of closed-region problems as it requires simpler model and yields modal *S*-parameters directly. Additionally, FEM matrix is filled only once for all frequencies as medium parameters are frequency independent. Nevertheless, we can conclude that the efficiency of the FEM approach is far more superior in this example; it requires almost 1/5 the number of unknowns and more than an order of magnitude less computational time than the MoM/SIE approach.

The second example is an inhomogeneous cubical scatterer in free space. The cube is lossless. It consists of three equally thick layers whose relative permittivities $(\varepsilon_r = \varepsilon_r')$ approximate linear change from $\varepsilon_r = 2$ to $\varepsilon_r = 4$ between two opposite faces. The cube is situated in vacuum and it is illuminated by a uniform plane wave incident along the direction of change of ε_r, as shown in Fig. 6. The cube is non-magnetic. This example demonstrates analysis of an open-region problem. Analysis by FEM requires the domain of interest to be properly bounded and truncated from the rest of the (infinite) space, which we do by means of the hybrid
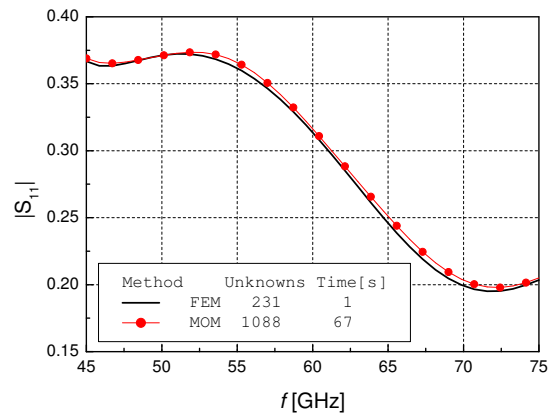
(a)
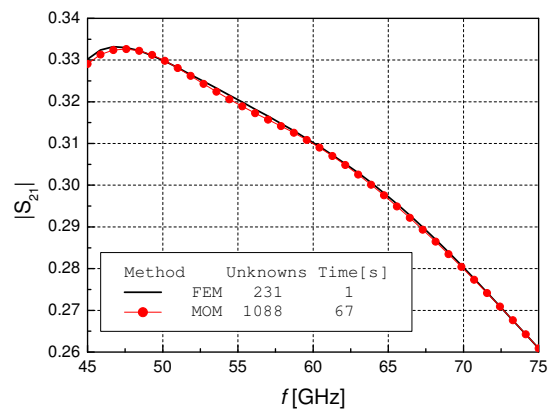
(b)

Fig. 5. *S*-parameters of the loaded WR-15 waveguide shown in Fig. 3; comparison of FEM (black curve) and MoM/SIE (red circles) results. Magnitudes of (a) S_{11} parameter and (b) S_{21} parameter.

higher order FEM-MoM; the fields within the cube are modeled by FEM and the domain is truncated at the cube faces by means of unknown surface currents which are evaluated by MoM [7,8]. The three layers of the cube are modeled by the three trilinear hexahedra in the FEM domain, visible in Fig. 6. In MoM domain, they are modeled by 14 bilinear quadrilaterals coinciding with the outer faces of the layers. The polynomial orders of the field approximations in FEM domain are 5 and

3 along the longer and shorter edges of the layers, respectively. The corresponding polynomial orders of the current expansion in MoM domain are 4 and 3 along the longer and shorter edges for all quadrilaterals (outer faces of the layers). The higher order hybrid FEM-MoM results will be compared with the solution obtained by the higher order MoM/SIE approach [6]. The MoM/SIE model consists of 16 bilinear quadrilaterals; the same 14 bilinear quadrilaterals comprising the outer boundary surface from Fig. 6 and additional two quadrilaterals (squares) positioned between the adjacent layers. Polynomial expansions for the surface currents in these models are optimally chosen and they range from 1 to 6 on different surfaces in different directions.
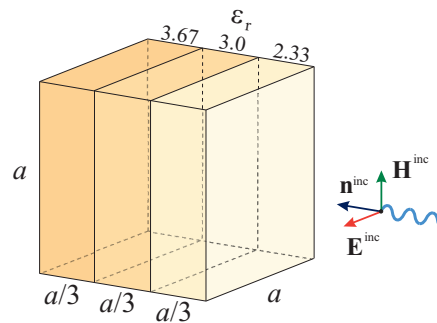

Fig. 6. Inhomogeneous lossless cubical scatterer in free space. The cube consists of three equally thick homogeneous layers optimally approximating linear change of ε_r. The figure describes models for both FEM-MoM and MOM/SIE analyses.

Fig. 7 shows the normalized radar cross section (RCS) of the cube against the normalized length of the cube side $4a/\lambda$, λ being the wavelength in the dielectric where $\varepsilon_r = 4$. It can be observed that the solution obtained by means of the higher order MoM/SIE is practically identical to the higher order FEM-MoM solution. The numbers of unknowns used in each of the analyses, shown in the figure legend, are as follows: hybrid FEM-MoM analysis employed 924 unknowns in the FEM region and 704 unknowns in the MoM region, MoM/SIE analysis employed 776 unknowns. Thus, in this example, the FEM-MoM solution employs approximately twice as many unknowns as the MoM/SIE solution (1628 combined FEM-MoM unknowns in the hybrid solution are needed compared to 776 unknowns in the MoM/SIE solution). The simulation times are also in favor of the MoM/SIE approach in this case. The MoM/SIE simulation lasted 85 s. The FEM-MoM simulation required 2.4 times more time, namely 209 s. This is primarily due to high FEM polynomial orders used for modeling of the fields in the cube interior and due to the complex nature of the hybrid FEM-MoM approach which simultaneously yields high-accuracy solution of the fields in the FEM domain. Nevertheless, we can conclude that the MoM/SIE approach is indeed superior to the FEM approach

in this example; it requires one half the number of unknowns and it is more than twice as fast as the FEM approach.
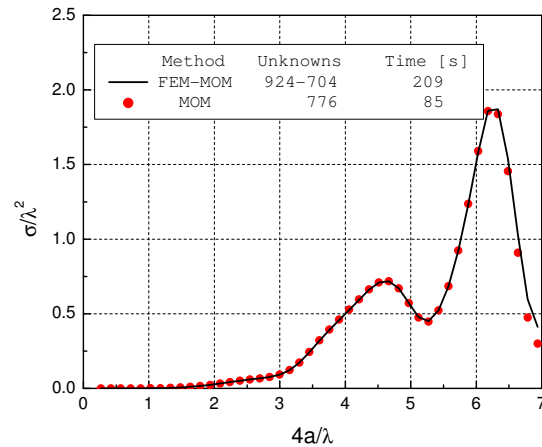

Fig. 7. Normalized RCS of the layered cubical scatterer shown in Fig. 6 against the normalized length of the cube side; comparison of hybrid FEM-MoM (black curve) and MoM/SIE (red circles) results.

4 Conclusions

We have investigated the efficiency of the higher order FEM and MoM/SIE modeling approaches in CEM by comparing their performances in two simple 3-D benchmark problems with similar meshes. The chosen examples demonstrate full-wave analysis of a wave-guiding structure (a closed-region problem) and a scatterer in free space (an open-region problem). Such a comparison has not been found in the open literature, probably because all of the commercially available FEM and MoM software packages (apart from WIPL-D) are essentially low order techniques.

We have evaluated the efficiency of the presented modeling approaches in two simple examples of closed-region and open-region EM problems involving inhomogeneous (and possibly lossy) dielectric bodies. The results obtained by the higher order large-domain FEM (hybridized with MoM for analysis of the open-region problem) have been compared with numerical results obtained by the higher order MoM/SIE approach. The examples have demonstrated that effective higher order FEM hexahedral meshes and MoM quadrilateral meshes, constructed from a very small number of large finite elements, could be applied even in the presence of the inhomogeneities. This has always been one of the strongest points

of the higher order modeling paradigm. It has been observed that, for the same accuracy, the presented FEM modeling approach required almost 1/5 the number of unknowns and more than an order of magnitude less computational time than MoM/SIE in the closed-region (loaded waveguide) example. In the open-region (scatterer in free space) example, it has been observed that the number of unknowns used by the presented hybrid FEM-MoM modeling approach was twice as high as that of the MoM/SIE and its computational time was 2.4 times longer than that of the MoM/SIE. Note, however, that significantly longer computational time of the hybrid FEM-MoM simulation in this example can partially be contributed to the complex nature of the hybrid method (which simultaneously yields high accuracy solution of the fields inside the FEM domain), but primarily to high FEM polynomial orders used for modeling of the fields in the scatterer interior. Based on the presented analysis, we can conclude that higher order FEM approach represents a method of choice in modeling of closed-region problems when effective large-domain volumetric meshing is available. At the same time, higher order MoM/SIE approach is the method of choice in modeling of open-region problems. Our future work will include a comparison of the two higher order approaches in analysis of partially closed and partially opened EM structures, such as cavity backed antennas and similar structures with radiating apertures, where the potential benefits of the hybrid method could be more pronounced.

Acknowledgments

References

[1] R. D. Graglia, D. R. Wilton, and A. F. Peterson, "Higher order interpolatory vector bases for computational electromagnetics," *IEEE Transactions on Antennas and Propagation*, vol. 45, no. 3, pp. 329–342, Mar. 1997.

[2] J. M. Jin, J. Liu, Z. Lou, and C. S. T. Liang, "A fully high-order finite-element simulation of scattering by deep cavities," *IEEE Transactions on Antennas and Propagation*, vol. 51, no. 9, pp. 2420–2429, Sept. 2003.

[3] M. M. Ilić and B. M. Notaroš, "Higher order hierarchical curved hexahedral vector finite elements for electromagnetic modeling," *IEEE Transactions on Microwave Theory and Techniques*, vol. 51, no. 3, pp. 1026–1033, Mar. 2003.

[4] M. M. Ilić, A. Z. Ilić, and B. M. Notaroš, "Higher order large domain FEM modeling of 3-D multiport waveguide structures with arbitrary discontinuities," *IEEE Transactions on Microwave Theory and Techniques*, vol. 52, no. 6, pp. 1608–1614, June 2004.

[5] B. M. Kolundžija, "Electromagnetic modeling of composite metallic and dielectric structures," *IEEE Transactions on Microwave Theory and Techniques*, vol. 47, no. 3, pp. 1021–1032, July 1999.

[6] M. Đorđević and B. M. Notaroš, "Double higher order method of moments for surface integral equation modeling of metallic and dielectric antennas and scatterers," *IEEE Transactions on Antennas and Propagation*, vol. 52, no. 8, pp. 2118–2129, Aug. 2004.

[7] X. Yuan, "Three-dimensional electromagnetic scattering from inhomogeneous objects by the hybrid moment and finite element method," *IEEE Transactions on Microwave Theory and Techniques*, vol. 38, no. 8, pp. 1053–1058, Aug. 1990.

[8] B. M. Notaroš, M. Đorđević, and M. M. Ilić, "Hybrid higher order techniques for CEM analysis and design," in *North American Radio Science Meeting - URSI 2007 digest*, Ottawa, Canada, 2007.

[9] B. M. Kolundžija, J. S. Ognjanović, and T. K. Sarkar, *WIPL-D: Electromagnetic Modeling of Composite Metallic and Dielectric Structures, Software and User's Manual.* Boston: Artech House, 2000.

[10] B. Kolundžija, B. Janić, and M. Rakić, "Novel technique for deembeding s-parameters in electromagnetic modeling of arbitrary circuits," in *Proceedings of IEEE AP-S International Conference, vol.3*, Monterey, California, USA, 2004, pp. 2784–2787.